Acta Crystallographica Section B
Structural Science
ISSN 0108-7681

Incommensurate crystallographic shear structure of $Ba_xBi_{2-2x}Ti_{4-x}O_{11-4x}$ ($x = 0.275$)

Yuichi Michiue,[a]* Akiji Yamamoto,[a] Mitsuko Onoda,[a] Akira Sato,[a] Takaya Akashi,[b]‡ Hisanori Yamane[c] and Takashi Goto[b]

[a]Advanced Materials Laboratory, National Institute for Materials Science, 1-1 Namiki, Tsukuba, Ibaraki 305-0044, Japan, [b]Institute for Materials Research, Tohoku University, Sendai 980-8577, Japan, and [c]Center for Interdisciplinary Research, Tohoku University, Sendai 980-8577, Japan

‡ Present address: Graduate School of Engineering, Hokkaido University, Sapporo 060-8628, Japan.

Correspondence e-mail: michiue.yuichi@nims.go.jp

Received 19 October 2004
Accepted 18 January 2005

The title compound generates diffraction patterns which are indexable within the framework of the higher-dimensional description of incommensurate structures. However, it is difficult to discriminate the main reflections from the satellite ones. This paper has clarified that the structure can be treated as a strongly modulated structure with sawtooth-like modulation functions and is classified as an incommensurate crystallographic shear (CS) structure. The structure consists of domains isostructural to β-$Bi_2Ti_4O_{11}$ and domain boundaries composed of TiO_6 octahedra. Ba and Bi ions are accommodated in the cavities between TiO_6 octahedra in the domain. Domain boundaries are aperiodically inserted, in contrast to the usual CS structures, forming an incommensurate structure.

1. Introduction

It is known that there are three typical structures showing incommensurate diffraction patterns: the modulated crystal (modulated structure), the composite crystal and the quasicrystal. For the first type we can easily recognize the main reflections on the lattice points of a three-dimensional reciprocal lattice since they are strong compared with other (so-called satellite) reflections. In the second case we can find several (usually two) sets of main reflections on the lattice points of the reciprocal lattices which are incommensurable with each other. They are accompanied by satellite reflections with a weak intensity. The existence of the main reflections requires that the point symmetry is crystallographic. On the other hand, in quasicrystals, the symmetry of the diffraction pattern is non-crystallographic and we cannot separate the main reflections from the satellite reflections. It is possible to consider the fourth case, where the main and satellite reflections are indistinguishable by the intensity distribution. The present compound shows such a character: in any choice of basic vectors for indexing, we cannot find strong main reflections.

A similar feature appears when composite crystals are treated as single modulated structures (Yamamoto, 1996), as recently shown for perovskite-related compounds (Elcoro *et al.*, 2003). When the intergrowth compounds with long unit-cell dimensions such as B-site-deficient perovskites (Elcoro *et al.*, 2000; Boullay *et al.*, 2003), Aurivillius phases (Boullay *et al.*, 2002*b*) and Ruddlesden-Popper phases (Elcoro *et al.*, 2001, 2004) are described as higher-dimensional crystals, we encounter the same situation. The common feature in these structures in their higher-dimensional models is the existence of the discontinuity in the modulation function. Such a modulation function is called a step-like occupation function

or a crenel function (Petříček *et al.*, 1995), which is called an occupation domain as in the quasicrystals in this paper. The non-existence of strong main reflections suggests that even if we can treat them as modulated structures, their modulation is very strong.

Several compounds exist which are closely related to the title compound. In the pseudoternary system BaO–Bi_2O_3–TiO_2, compounds belonging to the Aurivillius family are well known. They include $BaBi_4Ti_4O_{15}$, $Ba_2Bi_4Ti_5O_{18}$ (Aurivillius & Fang, 1962) and $BaBi_8Ti_7O_{27}$ (Subbanna *et al.*, 1990). Structures belonging to the family commonly contain perovskite layers separated by the $Bi_2O_2^{2+}$ layer. They are a special kind of superstructures which are known as intergrowth compounds. The existence of incommensurate phases has been reported for Aurivillius types in the peudobinary system Bi_3TiNbO_9–$Bi_4Ti_3O_{12}$ (Boullay *et al.*, 2002*a*), as well as for other layer structures in the systems Ti–S (Onoda & Wada, 1987), La–Ti–O (Van Tendeloo *et al.*, 1994) and so on. The structure analyses for these incommensurate structures have, however, not been carried out. A recent study for the phase relation in the BaO–Bi_2O_3–TiO_2 system at 1273 K revealed the existence of a new phase (Akashi *et al.*, 2001), which had an incommensurate character in the X-ray diffraction pattern and required four indices for the indexing of peaks. In this case it is difficult to use one of the usual procedures for modulated structure analysis, where an average structure is first solved by using the main reflections and after that the modulation functions are determined so as to explain satellite intensities. In this paper we applied the low-density elimination method (LDEM) to obtain an initial model for the structure refinement in order to avoid the difficulty in finding the average structure. This method gives an initial model in higher-dimensional (four-dimensional for the present case) space. This paper demonstrates the efficiency of the LDEM and clarifies the incommensurate structure of the title compound in detail.

2. Experimental

Single crystals were grown by the slow cooling method (Akashi *et al.*, 2001). Molar ratios estimated from the electron-probe microanalysis (EPMA) measurement of crystals were distributed between 5.16 and 6.15 for the Bi/Ba ratio, and between 0.45 and 0.50 for (Ba + Bi)/Ti. Crystallographic data, experimental conditions, and parameters for data collection and refinement are listed in Table 1.[1] The indexing by $h\mathbf{a}^* + k\mathbf{b}^* + l\mathbf{c}^* + m\mathbf{q}$ with $\mathbf{q} = \alpha\mathbf{a}^* + \gamma\mathbf{c}^*$ [$\alpha = 0.00005\ (8)$, $\gamma = 0.36693\ (3)$] showed systematic reflection conditions $h + k + l + m = 2n$ for $hklm$ (n: integer) due to the centering translation $(\frac{1}{2}, \frac{1}{2}, \frac{1}{2}, \frac{1}{2})$. This implies the superspace group is $I2/m(\alpha 1\gamma)$ or its non-centrosymmetric subgroup. This is equivalent to $B2/m(\alpha\beta 0)$ (No. 12.1; Janssen *et al.*, 1999) by, for example, $\mathbf{a}'^* = \mathbf{a}^*$, $\mathbf{b}'^* = \mathbf{a}^* + \mathbf{c}^*$, $\mathbf{c}'^* = -\mathbf{b}^*$, $\mathbf{q}' = \mathbf{q} - \mathbf{a}^*$ ($= -1.36693\mathbf{a}'^* + 0.36693\mathbf{b}'^*$). The symmetry operations of $I2/m(\alpha 1\gamma)$ with a conventional basis ($\mathbf{a}^*$, $\mathbf{b}^*$, $\mathbf{c}^*$, $\mathbf{q}$) are given by $(0, 0, 0, 0; \frac{1}{2}, \frac{1}{2}, \frac{1}{2}, \frac{1}{2}) + x_1, x_2, x_3, x_4; -x_1, x_2, -x_3, -x_4; -x_1, -x_2, -x_3, -x_4; x_1, -x_2, x_3, x_4$. The intensity distributions in the $h0lm$ and $h1lm$ planes are shown in Fig. 1. The grid shows the reciprocal lattice planes for the average structure chosen in this study.

3. Model building and structure refinement

In this study a four-dimensional superspace-group approach was applied to elucidate the structure of the new compound. From the intensity distribution mentioned in the previous section, it is easily conceivable that even if the structure is as tractable as a modulated structure, a conventional technique might not be applicable. In the common modulated structures,

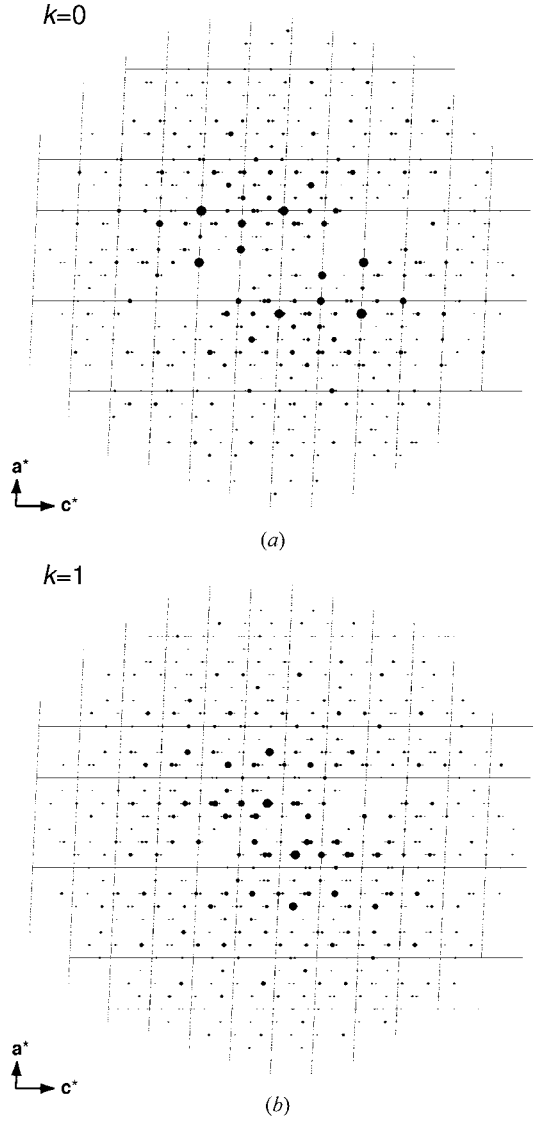

Figure 1
Representation of the diffraction pattern at (*a*) $k = 0$ and (*b*) $k = 1$ for $Ba_xBi_{2-2x}Ti_{4-x}O_{11-4x}$ ($x = 0.275$).

[1] Supplementary data for this paper are available from the IUCr electronic archives (Reference: SN5011). Services for accessing these data are described at the back of the journal.

Table 1
Crystallographic data and conditions for data collection and refinement.

Crystal data	
Chemical formula	$Ba_{0.0504}Bi_{0.2661}Ti_{0.6835}O_{1.8165}$
M_r	124.3
Cell setting, superspace group	Monoclinic, $I2/m(\alpha 1\gamma)$
a, b, c (Å)	10.6914 (3), 3.7963 (1), 3.3457 (1)
β (°)	92.625 (2)
$\mathbf{q}$ (= $\alpha\mathbf{a}^* + \gamma\mathbf{c}^*$)	0.00005 (8)$\mathbf{a}^*$ + 0.36693 (3)$\mathbf{c}^*$
V (Å^3)	135.65 (1)
Z	4
D_x (Mg m^{-3})	6.085 (1)
Radiation type	Nb $K\alpha$
Wavelength (Å)	0.7476
No. of reflections for cell parameters	4621
θ range (°)	2.5–45
μ (mm^{-1})	38.91
Temperature (K)	298
Crystal form, colour	Prism, pale yellow
Crystal size (mm)	0.10 × 0.05 × 0.04
Data collection	
Diffractometer	Mac Science DIP320
Data collection method	ω
Absorption correction	Empirical (using intensity measurements; Blessing, 1995)
T_{min}	0.161
T_{max}	0.274
No. of measured, independent and observed reflections	2389, 1059, 925
Criterion for observed reflections	$I > 2\sigma(I)$
R_{int}	0.033
θ_{max} (°)	45
Range of h, k, l, m	$-15 \Rightarrow h \Rightarrow 15$ $-4 \Rightarrow k \Rightarrow 3$ $-7 \Rightarrow l \Rightarrow 3$ $-4 \Rightarrow m \Rightarrow 4$
Refinement	
Refinement on	F
$R_{obs}(F)$, $wR_{obs}(F)$, S_{obs}	0.042, 0.042, 1.85
No. of reflections	925†
No. of parameters	81
Weighting scheme	Based on measured s.u.'s $w = 1/\sigma^2(F)$
$(\Delta/\sigma)_{max}$	0.006
$\Delta\rho_{max}$, $\Delta\rho_{min}$ (e Å^{-3})	3.08, −2.56
Extinction method	B-C type 1 Gaussian isotropic (Becker & Coppens, 1974)
Extinction coefficient	0.0027

Computer programs used: *JANA*2000 (Petříček & Dusek, 2000). † The 0200 reflection, which seems to suffer a strong extinction effect, was excluded from the refinement.

strong so-called main reflections form a three-dimensional lattice in the diffraction pattern. In the present case, however, such a lattice is difficult to find. Therefore, we chose, from many possibilities, one three-dimensional lattice and a corresponding modulation wavevector for indexing, which was eventually found to be the best for describing the structure as a simple layer sequence. As is clear from Fig. 1, the satellite intensity is sometimes stronger than that of the main reflections in any of the three-dimensional lattices.

In order to solve the problem we employed a direct method in higher-dimensional space, which was first applied to an icosahedral quasicrystal by extending the low-density modification method for complicated crystals, such as proteins (Shiono & Woolfson, 1992). The method uses random phases as the initial phases of independent reflections under an assumed space-group symmetry. The initial electron density given by the Fourier syntheses (Fourier transformation) generally shows positive and negative peaks. Provided that the minimum electron density of the Fourier map is the zero level, small peak heights were suppressed by the density modification function. The phases of the next cycle are calculated from the modified electron density by the inverse Fourier transformation. The electron density is calculated again by the Fourier synthesis. This cycle is repeated as often as the phases change. This method is based on the fact that the electron density is positive everywhere and it is almost flat, except in the vicinity of atoms, and peaks smaller than real atom peaks do not appear. This holds both in usual crystals and aperiodic crystals including modulated structures and quasicrystals. This was first applied to an icosahedral quasicrystal (Takakura *et al.*, 2001) by modifying a program for the usual crystals. An essential difference in the program is the space dimension,

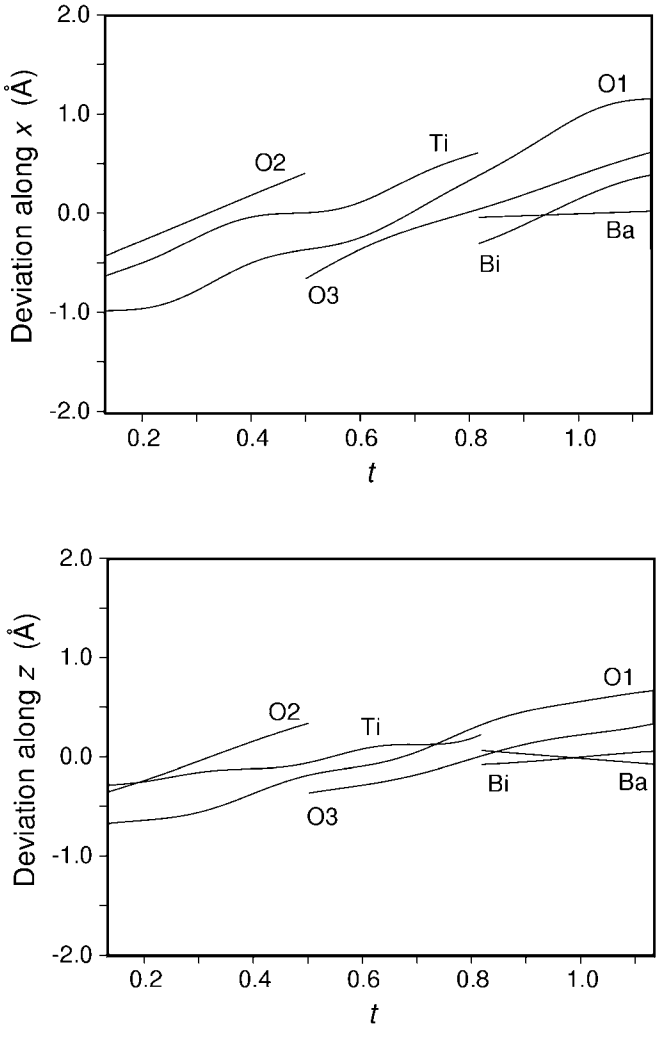

Figure 2
Deviations of atomic positions as functions of t (= $x_4 - \mathbf{q}\cdot\mathbf{r}_j$). No deviations are allowed in the direction of **b**.

Table 2
Structural parameters.

x_4^0 and Δ were given by the following

Bi: $x_4^0 = \gamma x_3^0 + (1-3\gamma)/4,\ \Delta = (1-\gamma)/2$
Ba: $x_4^0 = \gamma x_3^0 + (1-3\gamma)/4,\ \Delta = (1-\gamma)/2$
Ti: $x_4^0 = \gamma x_3^0 + 3(1-\gamma)/4,\ \Delta = (1+\gamma)/2$
O1: $x_4^0 = \gamma x_3^0 + 1 - \gamma,\ \Delta = 1$
O2: $x_4^0 = 1/2,\ \Delta = \gamma$
O3: $x_4^0 = \gamma x_3^0 - \gamma/2,\ \Delta = 1-\gamma$
$\gamma = 0.36693$.

V was set to 0.1Δ for x_1 and 0.2Δ for x_3 of the Ti and O atoms.

	Occupancy	x_1^0	x_2^0	x_3^0	x_4^0	Δ
Bi	0.8408	0.1029 (14)	0	0.755 (4)	0.2517 (13)	0.316535
Ba	0.1592	0.0822 (10)	0	0.689 (3)	0.2276 (16)	0.316535
Ti	1	0.358 (2)	0	0.711 (7)	0.736 (2)	0.683465
O1	1	0.2102 (4)	0	0.8802 (14)	0.9560 (5)	1
O2	1	0.5	0	0.5	0.5	0.36693
O3	1	0.589 (6)	0	0.760 (13)	0.096 (5)	0.63307

		x_1	x_2	x_3
Bi	V	0	0	0
	U_1^s	0.0080 (16)	0	−0.003 (4)
	U_1^c	−0.0387 (3)	0	−0.0236 (8)
Ba	V	0.003 (2)	0	−0.021 (6)
Ti	V	0.068347	0	0.136693
	U_1^s	−0.000 (4)	0	0.27 (11)
	U_1^c	−0.0134 (6)	0	−0.0483 (17)
	U_2^s	0.0016 (9)	0	−0.017 (3)
	U_2^c	0.001 (3)	0	−0.017 (8)
	U_3^s	−0.0007 (14)	0	−0.015 (4)
	U_3^c	0.0042 (9)	0	−0.001 (3)
O1	V	0.1	0	0.2
	U_1^s	0.0089 (5)	0	0.0226 (19)
	U_1^c	−0.0083 (7)	0	0.005 (2)
	U_2^s	−0.0032 (7)	0	−0.005 (2)
	U_2^c	−0.0054 (9)	0	−0.012 (3)
	U_3^s	0.0037 (11)	0	0.003 (3)
	U_3^c	0.0017 (13)	0	−0.007 (4)
O2	V	0.036693	0	0.073386
	U_1^s	−0.002 (2)	0	−0.033 (9)
	U_1^c	0	0	0
O3	V	0.063307	0	0.126614
	U_1^s	0.000 (6)	0	−0.011 (13)
	U_1^c	0.010 (8)	0	0.007 (18)
	U_2^s	−0.004 (5)	0	0.009 (11)
	U_2^c	−0.000 (2)	0	−0.011 (6)

		U^{11}	U^{22}	U^{33}	U^{12}	U^{13}	U^{23}	U_{eq}/U^{iso}
Bi	U_0	0.051 (6)	−0.037 (7)	0.023 (4)	0	0.015 (3)	0	0.012 (3)
	U_1^s	−0.048 (6)	0.111 (9)	−0.016 (4)	0	−0.018 (4)	0	
	U_1^c	−0.0090 (11)	0.0024 (19)	−0.0047 (8)	0	−0.0037 (7)	0	
Ba	U_0							0.0089 (15)
Ti	U_0	0.0044 (5)	0.0075 (8)	0.0058 (4)	0	−0.0012 (3)	0	0.0059 (3)
O1	U_0	0.0036 (15)	0.015 (3)	0.0085 (18)	0	−0.0008 (12)	0	0.0092 (13)
O2	U_0	0.001 (3)	0.018 (8)	0.0018 (6)	0	0.008 (4)	0	0.012 (4)
O3	U_0	0.010 (2)	0.012 (4)	0.0026 (18)	0	−0.0032 (15)	0	0.0084 (16)

The basic position is (x_1^0, x_2^0, x_3^0) and the occupation domain ranges from $x_4^0 - \Delta/2$ to $x_4^0 + \Delta/2$ in the fourth axis. Parameters for the modulation functions of the fractional coordinates u_j for the jth atom are given by (1)–(3) in the text. Parameters for anisotropic or isotropic displacement parameters $U_j^{\alpha\beta/iso}$ are given by (4).

which is 3 for crystals and 6 for icosahedral quasicrystals. A program for quasicrystals, which is only applicable to six-dimensional icosahedral quasicrystals, has been extended for use in three-dimensional to six-dimensional crystals (Yamamoto, 2004).

This method enables us to determine the different phases of the observed reflections. From the Fourier syntheses after the phase determination, atom positions emerged in four-dimensional space. We could easily distinguish metal atoms from O atoms in Fourier maps by peak heights. As in the usual modulated structures, each atom extends in the internal space, although its direction is not parallel to the fourth axis but nearly parallel to [1025] in the present case. Furthermore, the metal atoms extend within limited ranges. Some O-atom peaks were followed by metal-atom peaks along the [1025] direction. In order to refine such a structure, we needed to use stepwise or sawtooth-like modulation functions. In addition, detailed atom positions deviate from the straight line parallel to that direction. This necessitates additional positional modulation functions. We employed *JANA*2000 (Petříček & Dusek, 2000) in the structure refinement so as to use such modulation functions, where Fourier terms are applicable in addition to the sawtooth function. It was difficult to find the Ba site at the initial stage, but in the refinement process it was found that the Bi and Ba ions occupy almost the same (but slightly different) position, suggesting that they statistically occupy one cavity with an occupation probability less than one.

The position of each atom in four-dimensional space is specified by the four-dimensional coordinate x_i^0 $(i = 1, 2, 3, 4)$ of the atom and the range of the modulation function Δ along the fourth axis. Each modulation function is defined in the occupation domain which is the string passing through the point $\mathbf{x}^0 = (x_1^0, x_2^0, x_3^0, x_4^0)$ and ranging from $x_4^0 - \Delta/2$ to $x_4^0 + \Delta/2$ along the fourth axis. The positions of the occupation domains for independent atoms are shown in Table 2. Modulation functions for fractional coordinates u_j for the jth independent atom consist of two terms

$$u_j = u_{js} + u_{jh}. \quad (1)$$

The first term gives the sawtooth-like function which is essentially important for the present case. This is given by

$$u_{js} = (2V/\Delta)(\bar{x}_4 - x_4^0). \quad (2)$$

The second term gives an additional deviation expressed in terms of the Fourier series

$$u_{jh} = \Sigma_{n>0}[U_n^s \sin(2\pi n\bar{x}_4) + U_n^c \cos(2\pi n\bar{x}4)]. \quad (3)$$

The anisotropic or isotropic displacement parameter $U_j^{\alpha\beta/\mathrm{iso}}$ is also given in terms of the Fourier series including the zeroth-order term

$$U_j^{\alpha\beta/\mathrm{iso}} = U_{0j}^{\alpha\beta/\mathrm{iso}} + \Sigma_{n>0}[U_n^s \sin(2\pi n\bar{x}_4) + U_n^c \cos(2\pi n\bar{x}_4)]. \quad (4)$$

In the above equations, $\bar{x}_4$ is the fourth coordinate within the occupation domain. The coordinates x_i^0 ($i = 1, 2, 3, 4$), V, Δ and Fourier coefficients U_n^s and U_n^c in the above equations are refined parameters in the least-squares method, although many of them were fixed to specific values according to considerations explained later. Also, some parameters have to be fixed by the site symmetry at point $\mathbf{x}^0$. In the present case all atoms are on the mirror plane normal to **b**. This requires that x_2^0 coordinates of all atoms are zero or $\frac{1}{2}$ and U^{12} and U^{23} components of all Fourier coefficients of the anisotropic displacement parameters should be zero. Parameters U_n^c should be 0 for O2 at the inversion center. There are no additional conditions since the superspace group is planar monoclinic. Fourier coefficients up to the third order of the harmonic term u_{jh} have been taken into account for positional parameters of the Ti and O1 atoms (Table 2). The coefficients up to second order were refined for Bi and O3, and the first-order coefficients were for O2, while no harmonic modulation was taken for Ba. Anisotropic displacement parameters were used for all atoms except Ba. The first-order Fourier coefficients of the displacement parameters for Bi were refined, while no modulation of the displacement parameter was considered for other atoms. In the final stages some constraints for the parameters x_4^0 and Δ were necessary to avoid unrealistic local structures. Namely, Δ parameters were fixed to specific values and constraint conditions were imposed for x_4^0 so that the closeness condition (Cornier-Quiquandon *et al.*, 1992) is fulfilled in the final structure as in the analyses of quasicrystals.

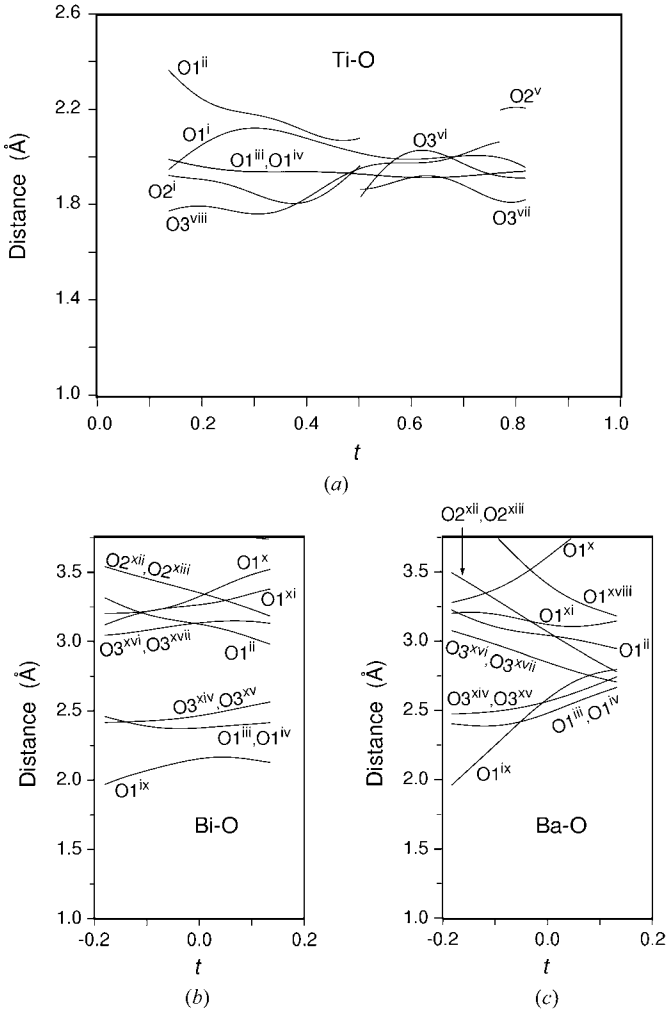

Figure 3
Interatomic distances for (*a*) Ti—O, (*b*) Bi—O and (*c*) Ba—O as functions of t ($= x_4 - \mathbf{q}\cdot\mathbf{r}_j$). Symmetry codes: (i) x_1, x_2, x_3, x_4; (ii) $x_1, x_2, x_3 - 1, x_4 - 1$; (iii) $-x_1 + \frac{1}{2}, -x_2 - \frac{1}{2}, -x_3 + \frac{3}{2}, -x_4 + \frac{3}{2}$; (iv) $-x_1 + \frac{1}{2}, -x_2 + \frac{1}{2}, -x_3 + \frac{3}{2}, -x_4 + \frac{3}{2}$; (v) $x_1, x_2, x_3 + 1, x_4 + 1$; (vi) $x_1, x_2, x_3, x_4 + 1$; (vii) $-x_1 + 1, -x_2, -x_3 + 1, -x_4 + 1$; (viii) $-x_1 + 1, -x_2, -x_3 + 2, -x_4 + 1$; (ix) $x_1, x_2, x_3, x_4 - 1$; (x) $x_1, x_2, x_3 + 1, x_4$; (xi) $-x_1, -x_2, -x_3 + 2, -x_4 + 1$; (xii) $x_1 - \frac{1}{2}, x_2 - \frac{1}{2}, x_3 - \frac{1}{2}, x_4 - \frac{1}{2}$; (xiii) $x_1 - \frac{1}{2}, x_2 + \frac{1}{2}, x_3 - \frac{1}{2}, x_4 - \frac{1}{2}$; (xiv) $x_1 - \frac{1}{2}, x_2 - \frac{1}{2}, x_3 + \frac{1}{2}, x_4 + \frac{1}{2}$; (xv) $x_1 - \frac{1}{2}, x_2 + \frac{1}{2}, x_3 + \frac{1}{2}, x_4 + \frac{1}{2}$; (xvi) $-x_1 + \frac{1}{2}, -x_2 - \frac{1}{2}, -x_3 + \frac{3}{2}, -x_4 + \frac{1}{2}$; (xvii) $-x_1 + \frac{1}{2}, -x_2 + \frac{1}{2}, -x_3 + \frac{3}{2}, -x_4 + \frac{1}{2}$; (xviii) $-x_1, -x_2, -x_3 + 1, -x_4 + 1$.

4. Results

4.1. Four-dimensional structure

The structure consists of one independent site for Bi, Ba and Ti atoms, and three oxygen sites for O1, O2 and O3, as shown in Table 2. The displacement parameter U^{22} of Bi is positive in the defined region, despite the negative U_0^{22} value. In Table 2 $2V/\Delta$ gives the tangent of the sawtooth function by the definition given in (2). The $2V/\Delta$ values of the Ti and O atoms were fixed to 0.2 for the x_1 coordinate and 0.4 for x_3, because these atoms are elongated almost parallel to the [1025] direction. This is also useful to prevent correlations between V and some Fourier coefficients in least-squares refinements. Deviations of atomic positions from the average values as functions of t ($= x_4 - \mathbf{q}\cdot\mathbf{r}_j$) are given in Fig. 2. Interatomic distances between the metal and nearest neighbour atoms are shown in Fig. 3 as functions of t. Ti—O distances are distributed between 1.75 and 2.37 Å (Fig. 3*a*), which is roughly similar to those in β-$Bi_2Ti_4O_{11}$ with Ti1—O between 1.789 (6) and 2.195 (7) Å, and Ti2—O between 1.884 (7) and 2.018 (4) Å (Kahlenberg & Bohm, 1995). The Bi ion is coordinated by five O ions forming a square pyramid ($O1^{iii}$, $O1^{iv}$, $O3^{xiv}$ $O3^{xv}$ at $x_2 = \pm\frac{1}{2}$ and $O1^{ix}$ at $x_2 = 0$) and additionally interacting with the second nearest group of seven O ions (Fig. 3*b*). This is basically identical to the situation in β-$Bi_2Ti_4O_{11}$ with five shorter Bi—O distances [one of 2.143 (4), two of 2.410 (5) and two of 2.464 (4) Å] and additionally seven longer ones [one of 3.146 (8), two of 3.141 (5), two of 3.299 (9) and two of 3.368 (1) Å]. The Ba ions are located at slightly deviated positions from those of the Bi

ion in the cavity. The coordination feature of the Ba ion is similar to that of the Bi ion in the lower t region, but changes according to the increase in t, as shown in Fig. 3(c). When t is near the upper limit, 0.13307 in Fig. 3(c), the Ba ion is in a distorted cube formed by eight O ions at $x_2 = \pm\frac{1}{2}$(O1^{iii}, O1^{iv}, O2^{xii}, O2^{xiii}, O3^{xiv}, O3^{xv}, O3^{xvi}, O3^{xvii}) and additionally surrounded by four O ions (O1^{ii}, O1^{ix}, O1^{xi}, O1^{xviii}) forming a distorted square on $x_2 = 0$. This coordination is similar to that of Ba1 in $BaTi_2O_5$ (Kimura *et al.*, 2003). Thus, the Ba ion in this region prevents the occurrence of short interatomic distances from O ions, which seems natural from the difference in ionic radii for the two ions: Ba 1.35, Bi 1.03 Å in six coordination and Ba 1.42, Bi 1.17 Å in eight coordination (Shannon, 1976). In order to check the validity of the obtained structure the bond-valence sums (BVSs; Brown & Altermatt, 1985) for Ti and Bi were calculated (Fig. 4). The values are roughly close to the expected ones; four for Ti and three for Bi. This confirms that the structure is crystallochemically natural. The calculated BVS for Ba was too large. This can, however, be understood as follows. From a crystallochemical point of view, a cavity occupied by a Ba ion should be expanded compared with that accommodating a Bi ion. Oxygen positions obtained from the refinement are the weighted means of the two cases; one is that the cavity is occupied by a Ba ion and another is by a Bi ion. The apparent cavity size is smaller than that accommodating the Ba ion because of the smaller ionic radius of the Bi ion than Ba. Thus, the calculated Ba—O distances which are shorter than the actual ones give the unlikely large BVS for Ba.

4.2. Three-dimensional structure

The structure in three-dimensional space is obtained from the four-dimensional structure discussed in the previous section by cutting it at a three-dimensional hyperplane normal to the internal space. Since the wavevector has no **b** component, the three-dimensional structure projected along **b** reveals a characteristic feature. (Fig. 5.) TiO_6 octahedra sharing edges or vertexes make up a framework structure in which the one-dimensional tunnel, that is the linear connection of cavities, extends along **b**. The cavity is occupied by the Bi ion which is partially replaced by the Ba ion. Their positions were slightly deviated from each other, although no Ba ion is shown in the figure for visibility. The structure is closely related to that of β-$Bi_2Ti_4O_{11}$ (Kahlenberg & Bohm, 1995). Domains isostructural to β-$Bi_2Ti_4O_{11}$ are found in the struc-

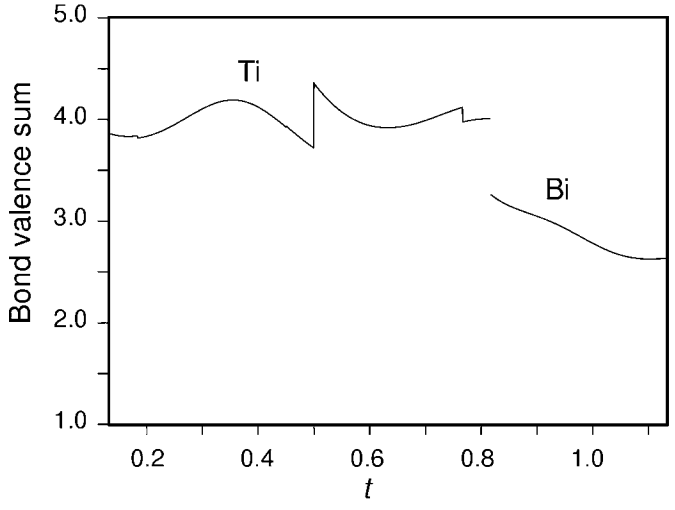

Figure 4
Bond-valence sum for Ti and Bi as functions of t ($= x_4 - \mathbf{q}\cdot\mathbf{r}_j$).

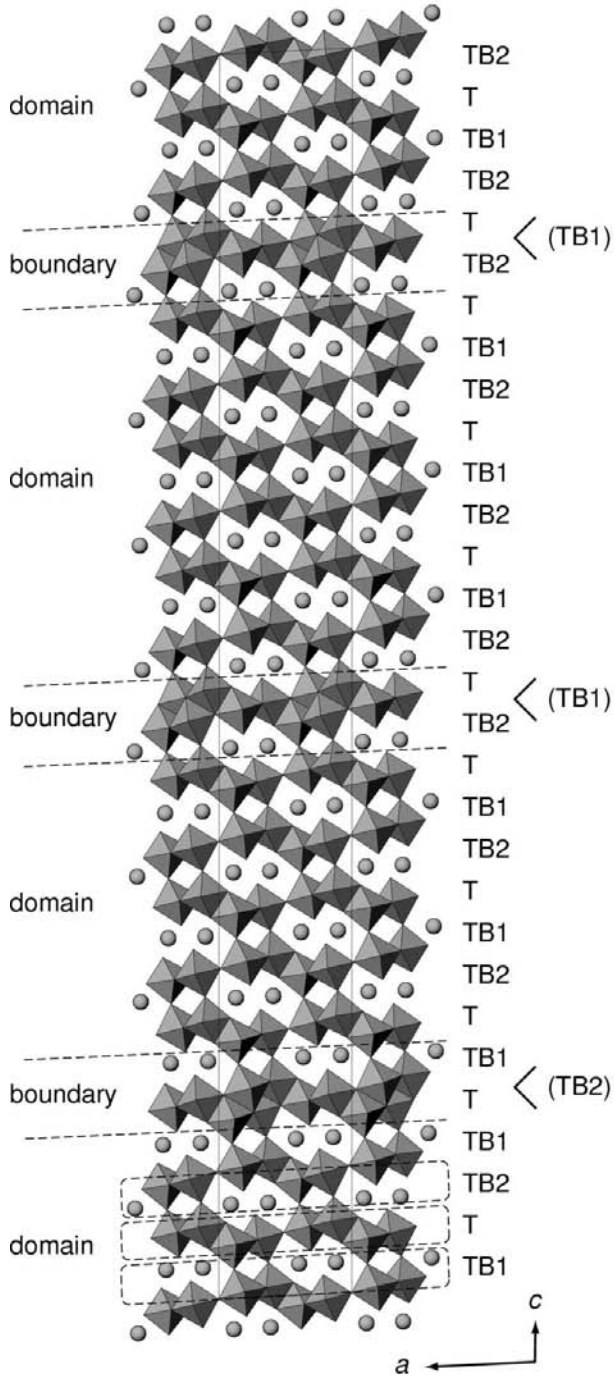

Figure 5
Partial structure of $Ba_xBi_{2-2x}Ti_{4-x}O_{11-4x}$ (x = 0.275) projected along **b**. The framework structure is represented by a linkage of TiO_6 coordination octahedra and the circles are Bi ions. T, TB1 and TB2 correspond to the regions in four-dimensional space as defined in Fig. 6.

ture, as indicated in Fig. 5, which are separated by the TiO_6-linkage layer which is thicker than that in the domain. The insertion of the thick TiO_6-linkage layer is understood from the four-dimensional structure as follows. In the unit cell in four-dimensional space, the Bi and Ba ions exist in the t range of a width *ca* 0.32, while the remaining *ca* 0.68 is allotted for Ti. The unit cell can be divided into three regions of t, which are shown as T, TB1 and TB2 in Fig. 6. The T region contains 4 Ti ions, while the TB region (or individually TB1 and TB2) includes the two Ti and two Bi (or Ba) ions. The sequence –TB1–T–TB2–, which makes up the β-$Bi_2Ti_4O_{11}$-like domain as shown in Fig. 5, is given from Fig. 6(*b*) by taking a cut along the external space (horizontal line). However, the TB layer is occasionally removed from the sequence giving different local structures –TB1–T–TB1–T–TB2– or –TB1–T–TB2–T–TB2–, because the width of the TB region in t is less than γ (= 0.36693). Thus, the thick TiO_6-linkage layer, or the domain boundary, is introduced into the structure. Furthermore, it was assumed that the width of the T region $\Delta(T)$ [$= 1 - 2\Delta(Bi)$] is equal to γ in order to avoid the appearance of unusual local structures –T–T– [in the case of $\Delta(T) > \gamma$] or –TB1–TB2–TB1–TB2– [$\Delta(T) < \gamma$]. This implies that the closeness condition is fulfilled as generally seen for intergrowth compounds (Elcoro *et al.*, 2003). From similar considerations along **a** (Fig. 6*a*) it was found that α should be 0, which is consistent with the experimental value within error. This led to a speculation that the chemical composition is determined by the modulation wavevector, which has been well established for many intergrowth polytypoids (Elcoro *et al.*, 2003, and references therein). Consequently, Δ parameters of the metal ions are related to the modulation wavevector by $\Delta(Bi) = (1 - \gamma)/2 = 0.316535$ and $\Delta(Ti) = (1 + \gamma)/2 = 0.683465$ or

$$\gamma = [\Delta(Ti) - \Delta(Bi)]. \qquad (5)$$

The estimated (Ba + Bi)/Ti ratio [$= \Delta(Bi)/\Delta(Ti) = 0.463$] is in agreement with the value given by the EPMA. The relation between the wavevector and the chemical composition is explicitly shown by the formula $(Ba,Bi)_{1-\gamma}Ti_{1+\gamma}O_{4-\gamma}$ or $Ba_{-1+3\gamma}Bi_{2-4\gamma}Ti_{1+\gamma}O_{4-\gamma}$ ($\frac{1}{3} \leq \gamma \leq \frac{1}{2}$) so as to maintain the charge neutrality. Therefore, the Bi/Ba ratio was set to $(2 - 4\gamma)/(-1 + 3\gamma) = 5.281$ in the refinement, which is consistent with the results from the EPMA measurement.

From the crystallochemical point of view, the present structure can be characterized as follows. The β-$Bi_2Ti_4O_{11}$-like domains separated by the thicker TiO_6-linkage layer seen in Fig. 5 occur with the introduction of the crystallographic shear (CS) operation illustrated in Fig. 7. This is achieved by the removal of two Bi, two Ti and eight O ions followed by the displacement of the block.[2] As the negative charge of a removed unit, $Bi_2Ti_2O_8^{2-}$, should be compensated by the substitution of the two Ba^{2+} ions for the two Bi^{3+} ions in the domains, the chemical composition of the whole structure is generally given by $Ba_{2\alpha}Bi_{2-4\alpha}Ti_{4-2\alpha}O_{11-8\alpha}$ [$= Bi_2Ti_4O_{11} - \alpha(Bi_2Ti_2O_8^{2-} + 2Bi^{3+} - 2Ba^{2+})$] or $Ba_xBi_{2-2x}Ti_{4-x}O_{11-4x}$ ($x = 2\alpha$). The latter formula means that the $\Delta(Ti)$ parameter should be equal to $(4 - x)/(6 - 2x)$ and $\Delta(Bi)$ to $(2 - x)/(6 - 2x)$, and the number of domain boundaries per unit cell is $x/(3 - x)$. Then from (5), the **c*** component of the modulation wavevector γ is given by $\gamma = 1/(3 - x)$ or $x = 3 - 1/\gamma = 0.2747$. The maximum of x is assumed to be 1. This corresponds to the hypothetical compound $BaTi_3O_7$ with $\gamma = \frac{1}{2}$, which is shown in Fig. 8. The number of domain boundaries per unit cell, $x/(3 - x)$ as mentioned above, is simply given by $3\gamma - 1$. The lower limit of γ, $\frac{1}{3}$, implies β-$Bi_2Ti_4O_{11}$ with no domain boundaries, while the upper one, $\frac{1}{2}$, gives $BaTi_3O_7$ in which TiO_6-linkage layers are all replaced by the thicker one as seen in Fig. 8.

5. Discussion

The layer sequence in intergrowth compounds is known to be closely related with the Fibonacci sequence and the Farey tree (Royal Society Mathematical Tables, 1950) because atom positions are given by occupation domains fulfilling the closeness condition similarly to quasicrystals. This was first demonstrated for compounds related to the 2H hexagonal perovskite (Perez-Mato *et al.*, 1999; Darriet *et al.*, 2002) and

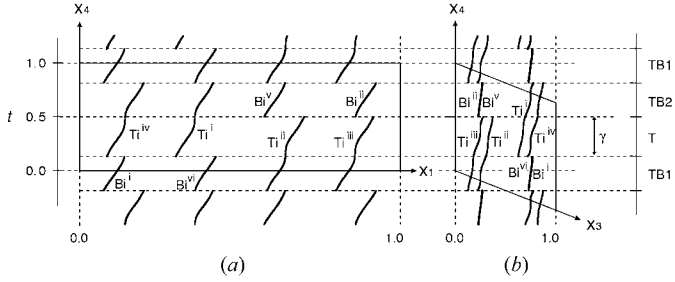

Figure 6
Ti and Bi atoms projected on x_1–x_4 and x_3–x_4 planes. Symmetry codes: (i) x_1, x_2, x_3, x_4; (ii) $1 - x_1, -x_2, 1 - x_3, 1 - x_4$; (iii) $x_1 + \frac{1}{2}, x_2 + \frac{1}{2}, x_3 - \frac{1}{2}, x_4 - \frac{1}{2}$; (iv) $-x_1 + \frac{1}{2}, -x_2 + \frac{1}{2}, -x_3 + \frac{3}{2}, -x_4 + \frac{3}{2}$; (v) $x_1 + \frac{1}{2}, x_2 + \frac{1}{2}, x_3 - \frac{1}{2}, x_4 + \frac{1}{2}$; (vi) $-x_1 + \frac{1}{2}, -x_2 + \frac{1}{2}, -x_3 + \frac{3}{2}, x_4 + \frac{1}{2}$.

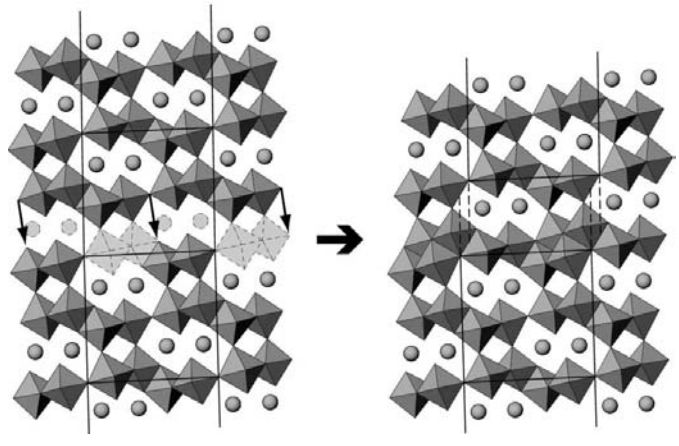

Figure 7
Schematic representation for the insertion of the domain boundary by the crystallographic shear operation.

[2] Only oxygen ions are removed in the usual CS operation, while metal and oxygen ions are removed in the present case. However, we regard the process in Fig. 7 as a kind of CS operation and call the derived structure the CS structure.

then applied for other structures such as B-site deficient perovskites (Elcoro *et al.*, 2000; Boullay *et al.*, 2003) and Aurivillius phases (Boullay *et al.*, 2002*b*). The same character is seen in the present CS structure, where γ is directly related to the term of the Farey tree. The β-$Bi_2Ti_4O_{11}$ structure ($\gamma = \frac{1}{3}$) corresponds to the term $\frac{1}{3}$ and the hypothetical $BaTi_3O_7$ ($\gamma = \frac{1}{2}$, Fig. 8) corresponds to $\frac{1}{2}$. Numerous structures with modulation wavevectors between $\gamma = \frac{1}{2}$ and $\cdots$ are deduced by just setting γ to a value between $\frac{1}{2}$ and $\cdots$ in the Farey tree and adjusting the parameters x_4^0 and Δ so as to maintain the closeness condition.

A series of fractions, 1/3, 3/8, 4/11, 7/19, 11/30,..., defined by $A_n/B_n = (A_{n-1} + A_{n-2})/(B_{n-1} + B_{n-2})$, with $A_1 = 1$, $B_1 = 3$, $A_2 = 3$, $B_2 = 8$, is seen in a part of the Farey tree and converges to $(\tau + 2)/(3\tau + 5) = 0.36716...$, where τ is the golden mean $(1 + 5^{1/2})/2$. As the observed γ value (= 0.36693) is between 11/30 and $(\tau + 2)/(3\tau + 5)$, it is of interest to compare structures of the three cases γ = 0.36693, 11/30 and $(\tau + 2)/(3\tau + 5)$. The three structures are identical in the area shown in Fig. 9 (within 30*c* along **c)**. In this region, the Farey tree rule (Perez-Mato *et al.*, 1999) is typically seen. Namely, the structure corresponding to the term 11/30 can be decomposed into two parts; one consisting of 19 unit cells and the other of 11. The former corresponds to the fraction 7/19 and the latter to 4/11. Further decomposition is possible until the elementary value of $\frac{1}{3}$ or $\frac{3}{8}$, as schematically shown in Fig. 9, although there are two types for the second fraction. If the structure is infinitely extended according to the Farey tree construction, that is by adding the structure of the preceding term, a hypothetical structure with the wavevector $\gamma = (\tau + 2)/(3\tau + 5) = 0.36716...$ is obtained. Namely, the 11/30 structure is extended to the 18/49 structure by adding 7/19 and 18/49 is further extended to 29/79 by adding 11/30, and so forth. On the other hand, the mere repetition of the 11/30 structure gives the superstructure of γ = 11/30. The present structure with $\gamma = 0.36693$ is not identical to either of the two structures. A few differences between these three cases are revealed by comparing the structures of 90 times the unit cell, which is given as a supplementary material.

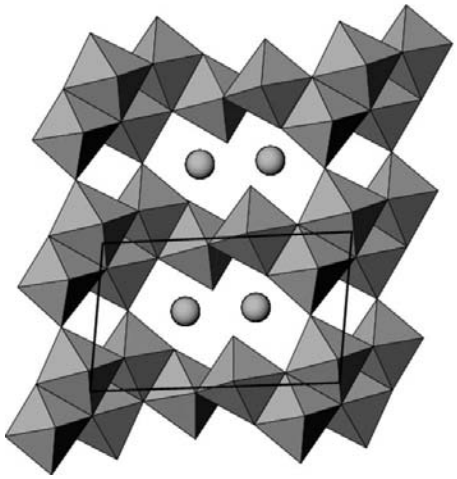

Figure 8
Hypothetical structure of $BaTi_3O_7$ with $\gamma = 1/2$. The origin is shifted by ($\frac{1}{4}$, $\frac{1}{4}$, $\frac{1}{4}$, $\frac{1}{4}$).

The β-$Bi_2Ti_4O_{11}$ structure is the high-temperature phase in the $Bi_2Ti_4O_{11}$ compound and transforms to the antiferroelectric α-$Bi_2Ti_4O_{11}$ by the antiparallel displacement of Bi ions along **b** at 506 K (Kahlenberg & Bohm, 1995). In the present structure, however, the substitution of the smaller divalent cation such as Ca or Sr for Ba will be necessary to realise such a phase transition, because the Ba ion is too large to shift in the cavity. Each β-$Bi_2Ti_4O_{11}$-like domain might be stabilized by the displacement of the cations in the tunnel, while interactions between the domains must be complicated. On the other hand, the existence of other commensurate phases in addition to β-$Bi_2Ti_4O_{11}$ ($\gamma = \frac{1}{3}$) is expected. Superstructures with γ = 3/8 or γ = 4/11 are strongly suggested, where the 3/8 or the 4/11 unit in Fig. 9 is merely repeated.

In summary, it has been clarified that the incommensurate structure of $Ba_xBi_{2-2x}Ti_{4-x}O_{11-4x}$ (x = 0.275) is closely related to the β-$Bi_2Ti_4O_{11}$ structure (Kahlenberg & Bohm, 1995), which contains the one-dimensional tunnel, or a linear sequence of cavities, occupied by the Bi ion. In addition to the partial substitution of Ba ions for Bi ions in the tunnel, domain boundaries parallel to the tunnel direction are introduced by the CS operation. The unique character of the structure is the aperiodic insertion of the domain boundaries, which may appear to be irregular at first sight, but is actually defined by

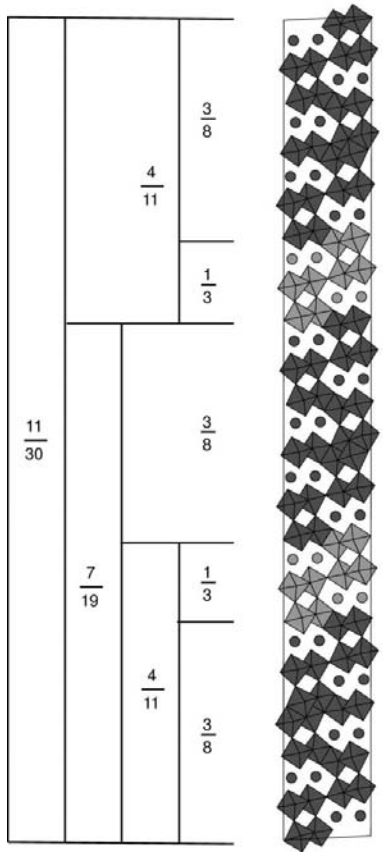

Figure 9
Construction of the partial structure of $Ba_xBi_{2-2x}Ti_{4-x}O_{11-4x}$ (x = 0.275) of 30 times the unit cell along **c**. The lighter shading is the elementary unit of $\frac{1}{3}$ and the darker shading is that of $\frac{3}{8}$.

the conventional four-dimensional formalism; the three-dimensional section of a periodic four-dimensional structure consisting of occupation domains. To the best of our knowledge, this is the first example of the quantitative analysis of the incommensurate CS structure with no *a priori* structure model.

References

Akashi, T., Morita, K., Hirai, T., Yamane, H. & Goto, T. (2001). *Mater. Trans.* **42**, 1823–1826.

Aurivillius, B. & Fang, P. H. (1962). *Phys. Rev.* **126**, 893–896.

Becker, P. J. & Coppens, P. (1974). *Acta Cryst.* A**30**, 129–147.

Blessing, R. H. (1995). *Acta Cryst.* A**51**, 33–38.

Boullay, P., Trolliard, G., Mercurio, D., Perez-Mato, J. M. & Elcoro, L. (2002*a*). *J. Solid State Chem.* **164**, 252–260.

Boullay, P., Trolliard, G., Mercurio, D., Perez-Mato, J. M. & Elcoro, L. (2002*b*). *J. Solid State Chem.* **164**, 261–271.

Boullay, P., Teneze, N., Trolliard, G., Mercurio, D. & Perez-Mato, J. M. (2003). *J. Solid State Chem.* **174**, 209–222.

Brown, I. D. & Altermatt, D. (1985). *Acta Cryst.* B**41**, 244–247.

Cornier-Quiquandon, M., Gratias, D. & Katz, A. (1992). *Methods of Structural Analysis of Modulated Structures and Quasicrystals*, edited by J. M. Perez-Mato, F. J. Zuniga & G. Madariaga, pp. 313–332. Singapore: World Scientific.

Darriet, J., Elcoro, L., El Abed, A., Gaudin, E. & Perez-Mato, J. M. (2002). *Chem. Mater.* **14**, 3349–3363.

Elcoro, L., Perez-Mato, J. M., Darriet, J. & El Abed, A. (2003). *Acta Cryst.* B**59**, 217–233.

Elcoro, L., Perez-Mato, J. M. & Withers R. L. (2000). *Z. Kristallogr.* **215**, 727–739.

Elcoro, L., Perez-Mato, J. M. & Withers R. L. (2001). *Acta Cryst.* B**57**, 471–484.

Elcoro, L., Zuniga, F. J. & Perez-Mato, J. M. (2004). *Acta Cryst.* B**60**, 21–31.

Janssen, T., Janner, A., Looijenga-Vos, A. & de Wolff, P. M. (1999). *International Tables for Crystallography*, Vol. C, edited by A. J. Wilson, pp. 899–947. Dordrecht: Kluwer Academic Publishers.

Kahlenberg, V. & Bohm, H. (1995). *Acta Cryst.* B**51**, 11–18.

Kimura, T., Goto, T., Yamane, H., Iwata, H., Kajiwara, T. & Akashi, T. (2003). *Acta Cryst.* C**59**, i128–i130.

Onoda, M. & Wada, H. (1987). *J. Less-Common Met.* **132**, 195–207.

Perez-Mato, J. M., Zakhour-Nakhl, M., Weill, F. & Darriet J. (1999). *J. Mater. Chem.* **9**, 2795–2808.

Petříček, V. & Dusek, M. (2000). *JANA*2000. Institute de Physics, Praha, Czech Republic.

Petrícek, V., van der Lee, A. & Evain, M. (1995). *Acta Cryst.* A**51**, 529–535.

Royal Society Mathematical Tables (1950). *The Faraday Series of Order 1025*, Vol. I. Royal Society/Cambridge University Press.

Shannon, R. D. (1976). *Acta Cryst.* A**32**, 751–767.

Shiono, M. & Woolfson, M. M. (1992). *Acta Cryst.* A**48**, 451–456.

Subbanna, G. N., Gururow, T. N. & Rao, C. N. R. (1990). *J. Solid State Chem.* **86**, 206–211.

Takakura, H., Shiono, M., Sato, T. J., Yamamoto, A. & Tsai, A. P. (2001). *Phys. Rev. Lett.* **86**, 236–239.

Van Tendeloo, G., Amelinckx, S., Darriet, B., Bontchev, R., Darriet, J. & Weill, F. (1994). *J. Solid State Chem.* **108**, 314–335.

Yamamoto, A. (1996). *Acta Cryst.* A**52**, 509–560.

Yamamoto, A. (2004). Unpublished.